High-Accuracy Product Life Estimation of GaN-HEMT by μ–Raman and Numerical Simulation

Takumi YONEMURA*, Masato FURUKAWA, Shinya MIZUNO, Shinji MATSUKAWA, Manabu SHIOZAKI, and Yasuo NAMIKAWA

High-efficiency and high-frequency GaN-HEMTs (gallium-nitride high-electron-mobility transistors) for satellites and mobile phone base stations need to assure long-term reliability. The life time of these products is estimated based on the temperature of the channel layer (Tch), with a channel length of approximately 0.2 μm, located under the gate electrode. However, the current measurement method using an infrared microscope with a spatial resolution of 4 μm is insufficient to obtain the Tch precisely. We have developed a high-accuracy estimation method that uses μ-Raman spectroscopy with a spatial resolution of 0.8 μm, and achieved an accuracy of ± 5 degrees C by the optimization of sample structures for μ-Raman spectroscopy and careful calibration. It was confirmed that the life time of our existing products estimated by this method is 20 times longer than that estimated by the infrared microscope measurement on the same Tch.

Keywords: GaN-HEMT, channel temperature, product lifetime, Raman spectroscopy, numerical simulation

1. Introduction

Gallium nitride (GaN) is a well-known wide-gap semiconductor material, which is utilized in many devices such as high-efficiency and high-frequency electronic devices. These devices contribute to realize an information society where the transmission rate and quantity of information are increasing rapidly. Sumitomo Electric Industries, Ltd. has developed and released GaN high-electron mobility transistors (GaN HEMTs*1) for several band frequency ranges of up to 80 GHz. They have been mounted into mobile phone base stations, communication satellites, and other equipment.

In such equipment, it is especially important to guarantee the long-term reliability of GaN-HEMT devices because it is difficult to replace them once they are mounted. The lifetime of GaN-HEMTs has conventionally been estimated based on their channel temperature, T_{ch}, which is defined as the surface temperature of these devices observed by an infrared microscope during operating. However, it is necessary to measure the temperature of a highly heated local region inside the device and define the measured value as T_{ch} to estimate the lifetime more accurately. Recently, numerical analysis and Raman spectroscopy*2 with a spatial resolution of less than one μm have been studied as T_{ch} measurement methods instead of an infrared microscope.[1]-[3] However, few papers have discussed the accuracy of T_{ch} that was measured by the above mentioned methods.

We improved the measurement accuracy of T_{ch} by combining Raman spectroscopy and numerical analysis, and investigated the original measurement accuracy of this method. Then we optimized the measurement sample structure for Raman spectroscopy and applied a careful calibration. As a result, we have developed a new technique that can measure T_{ch} to an accuracy of 5°C or less with a spatial resolution of 0.8 μm. This paper describes the features and performance of the new technique.

2. Operating Principle and Lifetime of GaN-HEMT

2-1 Operating principle

A GaN-HEMT device generally has an AlGaN/GaN transistor structure that is epitaxy grown on a silicon carbide (SiC) substrate as shown in Fig. 1. A high-mobility two-dimensional electron gas (2DEG) layer is formed near the boundary between GaN and AlGaN. An electric current flows through the 2DEG layer when the voltage is applied between the source and drain. The amount of the current is controlled by applying voltage to the gate that forms the channel layer under the gate.

2-2 Lifetime estimation method for GaN-HEMT and problems to be solved

During the device operation, most of the Joule heating occurs at an approximately 0.2 μm long area in the GaN layer below the gate, and the temperature at this region is to be maximum. It is necessary to measure this temperature (T_{ch} at point ★ in Fig. 1) to estimate the lifetime accurately.

However, a conventional method using an infrared microscopy with a spatial resolution of 4 μm fails to measure T_{ch} accurately, because the spatial resolution is larger than the measured region between the drain and source[4] and the silicon nitride (SiN), electrodes, and other materials on the GaN layer also make the measurement accuracy lower. In addition, it is difficult to measure the high temperature area under the gate electrode because it

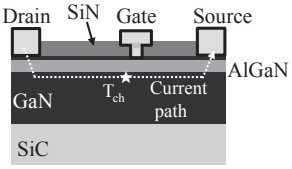

Fig. 1. Schematic illustration of GaN-HEMT

is covered by the electrode metal. To overcome above problems, we developed a method that combines numerical analysis and Raman spectroscopy with a spatial resolution of 0.8 μm. Raman spectroscopy can selectively extract the temperature of the GaN layer and numerical analysis makes it possible to estimate the temperature distribution in the area covered with an electrode.

3. Measurement Technique and Improvement of Quantitative Determination Accuracy

3-1 Outline of T_{ch} determination method

Raman spectroscopy is a method using Raman scattering, which is generated by the interaction of the irradiated laser beam with molecular vibration or phonons. Sample temperature can be derived from analyzing the frequency shift of Raman scattering. Since the intensity of the irradiated laser beam follows the Gaussian distribution, the intensity of the Raman scattering having the frequency corresponding to the temperature of the irradiation center will be maximized. This means that the measured temperature is not the average temperature of the area irradiated with the 0.8 μm diameter laser beam, but the temperature at the irradiation center. As shown in Fig. 2, we measured the temperature of GaN layer at the center position (R_{cen}) between the gate and drain (T_{Ra} (R_{cen})) with Raman spectroscopy by the laser beam through the transparent SiN film. On the other hand, the temperature below the electrodes cannot be measured by Raman spectroscopy because the irradiated laser beam is blocked. Therefore, we simulated the distribution of temperature below electrode using numerical analysis. We calculated the temperature difference (ΔT_{CAE}) between R_{cen} and the end portion R_G of the gate, and determined T_{ch} by adding ΔT_{CAE} to T_{Ra} (R_{cen}) ($T_{ch} = T_{Ra}$ (R_{cen}) + ΔT_{CAE}).

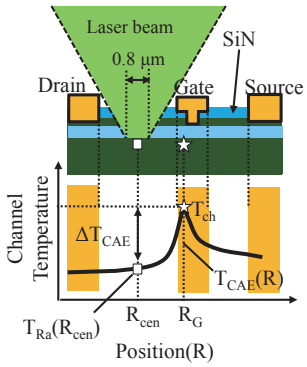

Fig. 2. Determination method of T_{ch}

3-2 Improvement of the temperature measurement accuracy on Raman spectroscopy

(1) Outline of temperature measurement using Raman spectroscopy

The change of the temperature or polarization state of the specimen causes a frequency shift of Raman scattering.[2),5)] To measure the channel temperature of a device in operation, it is necessary to investigate a relationship between the frequency and specimen temperature, namely, calibration curve including the inverse piezoelectric effect*3 induced by the applied voltage. Therefore, a calibration curve was prepared under the condition that the voltage was applied between the drain and source.

(2) Measurement system and specimen

The measurement system is schematically illustrated in Fig. 3. Raman spectroscopy was conducted using an HR-800 model made by Jobin Yvon Inc. and a YAG laser excitation source (532 nm, 5 mW), using a pinhole (diameter = 100 μm) and a long focus hundredfold object lens whose numerical aperture (NA) is 0.6 to focus the laser onto the device and to collect the Raman scattering. The spatial resolution was confirmed as 0.8 μm by a knife-edge method*4 using an indium phosphide (InP) with a cleavage face.

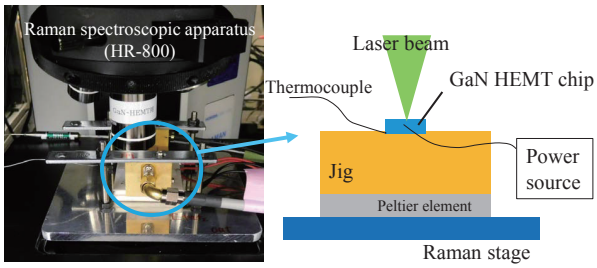

Fig. 3. Schematic illustration of measurement system

The specimen, a GaN-HEMT chip package, was fixed to the jig at both sides with two screws as shown in Fig. 4. A thermocouple is attached to a point 2 mm outside the outer periphery of the chip as in a conventional reliability test. The temperature measured by the thermocouple is defined as the chip temperature (T_b). A Peltier element was sandwiched between the stage and jig as shown Fig. 3 to control T_b within a range of 50 to 100°C.

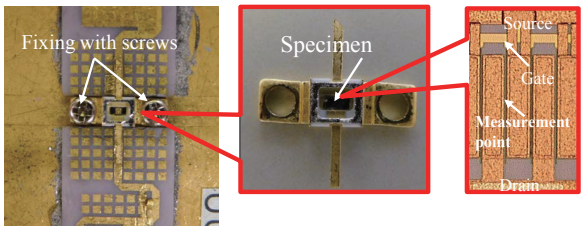

Fig. 4. Fixation method for GaN-HEMT chip and its enlarged views

In this paper, two specimens with different distances between the gate and drain (L_{gd}) (A: L_{gd} = 2 μm, B: L_{gd} = 5 μm) were prepared. To prevent the electrodes connected to

the drain and source from blocking the incident laser beam on Raman spectroscopy, the electrodes were designed not to interfere with the incident laser beam taking into account of the NA of the object lens as shown in Fig. 5. It was confirmed by the numerical analysis described later that the influence of the change of the electrode structure to the measured temperature was less than 1°C.

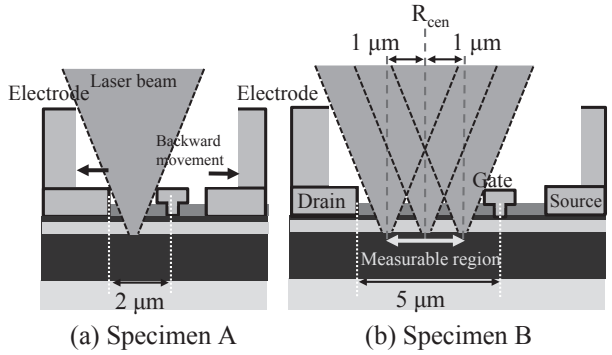

Fig. 5. Relationship between the sample structure and laser beam and laser beam

For specimen A, whose L_{gd} was 2 μm, Raman spectroscopy was effective at only one point of R_{cen} between the gate and drain. In contrast, for specimen B, whose L_{gd} was 5 μm, temperature distribution in the range of R_{cen} ± 1 μm was measurable. By comparing the measured temperatures and those obtained from numerical analysis, and by fitting the parameters of the numerical analysis model, L_{gd} variable numerical model was optimized. The bias condition for the Raman spectroscopy was set at V_{ds} = 26 V and I_{ds} = 150 mA.

(3) Investigation and improvement of measurement accuracy

We picked out factors that influence the measurement accuracy on Raman spectroscopy and quantified them. The factors were grouped into the following four categories:

1. Fluctuation of measured temperature due to variation of thermocouple contact force
2. Fluctuation due to variation in specimen and jig setting accuracies
3. Fluctuation of measured value (during the day/daily) due to change in outside environment
4. Fluctuation of measurement accuracy intrinsic to apparatus (repeatability)

Table 1 shows the measurement accuracy for above each factor 1 through 4. It was found that the total measurement accuracy was approximately 25°C and this value was larger than the measurement error (4°C) intrinsic to apparatus (repeatability), which is item 4 in Table 1. To improve the total measurement accuracy, a calibration technique was applied. We performed Raman spectroscopy for specimen A under the condition same as the calibration curve measurement, and determined the difference Δ between the measured temperature and that of calibration curve. The channel temperature of device in operation was corrected using Δ. Figure 6 shows the relationship between T_b and T_{Ra} (R_{cen}). It was found that T_b is highly proportional to T_{Ra} with a correlation coefficient (R^2) of 0.92. This indicates that the measurement accuracy of T_{Ra} (R_{cen}) had been improved to less than 5°C.

Table. 1. Variable factors in Raman spectroscopy and investigation of the effect of these factors on measurement accuracy

	Variable factor	Check point	Variation
1	Variation in thermocouple contact force	Investigation of variation by repeatedly attaching thermocouple to specimen	1°C
2	Variation in specimen setting accuracy	Investigtion of variation by repeatedly setting specimen	10°C
3	Variation due to change in outside environment	Investigation of variation several times (morning, evening, and daytime) without removing specimen	10°C
4	Repeatability	Investigation of variation by repeatedly measuring at the same point	4°C

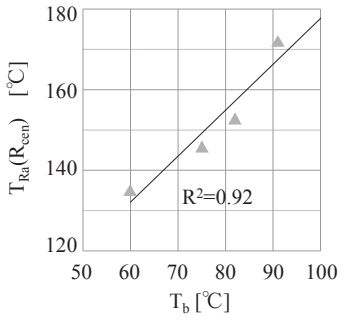

Fig. 6. Correlation between chip temperature (T_b) and temperature measured by Raman spectroscopy (T_{Ra} (R_{cen}))

3-3 Estimation of temperature distribution inside device by numerical analysis

(1) Dominant parameter selection in spatial distribution of temperature

We used commercial device simulation software, SILVACO ALTAS, to calculate the spatial distribution of temperature in device operation.[6] This software can be used to calculate the detailed temperature distribution inside a device through an analysis taking the spatial distribution of electric field, carrier transport, self-heating, and other factors into account.

Mobility, band gap, electron affinity, and many other physical properties of each material are required for its simulation. However, these parameters don't affect the temperature distribution under the conditions for this study where the amount of heat generated inside the device can be determined from the product of V_{ds} and I_{ds}.

Thermal conductivity is only the parameter that affects the temperature distribution and the parameter of each material reported in several references.[7]-[12] However, in these references, the several values within a range of approximately 20% were suggested. Therefore, we investigated their effect on ΔT_{CAE} varying the value of the thermal conductivity of SiC, GaN, AlGaN, and SiN, which are the principal materials of the device, within a range of ±20%. As a result, it was found that the influence of the variation of the thermal conductivity of SiC, AlGaN, and SiN on the temperature distribution was 0.5°C or less. In contrast, the

effect of GaN was 3°C, which was larger than the effect of other materials. This result indicates that we should select the appropriate value of the thermal conductivity of GaN from the values of their references. Therefore, we decided to use thermal conductivity of GaN as a fitting parameter for agreement with experimental results.

(2) Determination of the thermal conductivity of GaN

We used specimen B for the determination of the thermal conductivity of GaN. Based on the comparison of the temperature gradients measured by Raman spectroscopy and numerical analysis, the thermal conductivity of GaN was determined to be 1.3 W/m•K. In this process, the area between the measurement jig and chip back surface was excluded from the analysis domain. Instead, a thermal resistance of 7.9 K/W, which was determined from a 3D finite element analysis, was given as a boundary condition. The thermal conductivities of the other three materials used for the numerical analysis are shown in Table 2.

Table. 2. Thermal conductivities used for simulation

Material	Thermal conductivity [W/m•K]
SiN	0.185
AlGaN	0.19
GaN	1.3
SiC	5.2

The temperature distribution obtained by the above method is shown in Fig. 7. This figure shows that the edge immediately beneath the gate on the drain side is heated most severely. Figure 8 compares Raman spectroscopy and numerical calculation results for temperature gradient in the measurable range (1.8 - 3.8 μm). In this figure, the distance from the center of the gate is plotted on the horizontal axis and the 2DEG temperature calculated by numerical analysis on the vertical axis. As seen from this figure, the temperature gradients obtained by both techniques were in good agreement with each other.

In the following section, we discuss the temperature difference ΔT_{CAE} between the measurement point for Raman spectroscopy R_{cen} and the maximum temperature point in 2DEG using the new measurement technique.

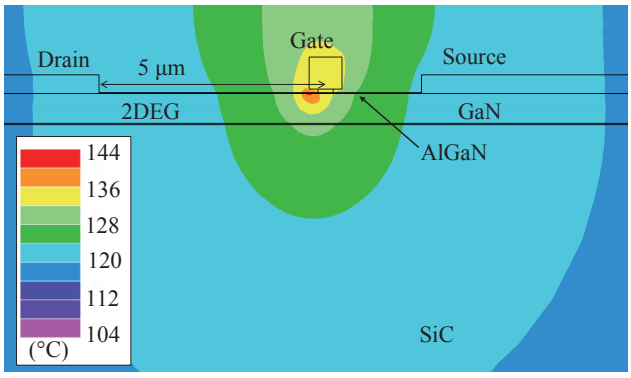

Fig. 7. Numerical simulation result for temperature distribution in specimen B

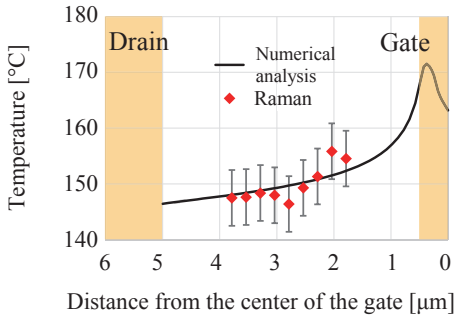

Fig. 8. Comparison of temperature gradients obtained by Raman spectroscopy and numerical analysis

4. Result and Discussion

Figure 9 shows the comparison of the channel temperature obtained by this new technique combined Raman spectroscopy and numerical analysis and by the conventional one with an infrared microscopy. T_{ch} measured by the new technique of 200°C was higher by 35°C than that measured by the infrared microscope method of 165°C for the same T_b. This temperature difference was considered that T_{ch} was underestimated in the infrared microscopy measurement due to averaging of the temperature around T_{ch}.

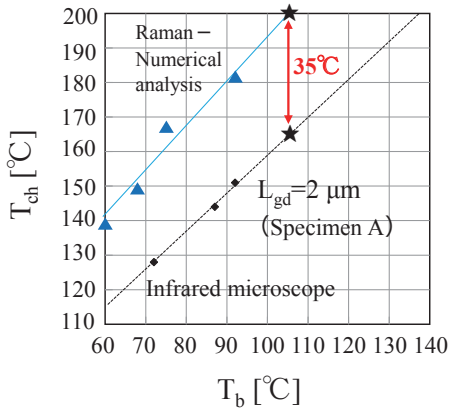

Fig. 9. Comparison of Tch obtained by Raman-numerical analysis and by an infrared microscopy

Figure 10 shows the relationship between T_{ch} and the lifetime of our existing products. The lifetime is represented in terms of mean time to failure (MTTF). The broken line in Fig. 10 shows the temperature dependence of MTTF obtained by an infrared microscopy, while the solid line in Fig. 10 shows one estimated by using the above result. The MTTF at T_{ch} = 200°C was estimated to be 1×10^6 hours using the result obtained by infrared micros-

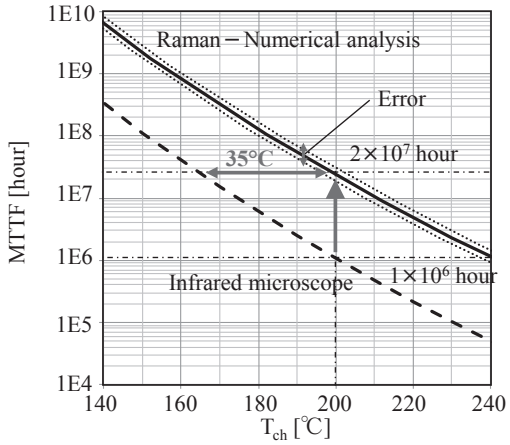

Fig. 10. Comparison of the MTTF of our product estimated by Raman-numerical analysis and by an infrared microscopy

copy. In contrast, the MTTF was estimated to be 2×10^7 hours using that obtained by the new technique. In short, the lifetime of our existing products estimated by the new technique is confirmed to be 20 times longer than that estimated by the infrared microscopy on the same T_{ch}.

5. Conclusion

Aiming to apply the T_{ch} measurement method that combines Raman spectroscopy and numerical analysis to estimate the lifetime of our products more accurately, we investigated the variable factors that affect the measurement accuracy, optimized the specimen structure, and conducted calibration. As a result, we have developed a new technique that can measure T_{ch} to an accuracy of 5°C with a spatial resolution of 0.8 μm. It has been confirmed that the lifetime of our products estimated by this new technique is 20 times longer than that estimated by the infrared microscopy on the same T_{ch}.

6. Acknowledgments

We are grateful to Mr. Shigeru Kuroda, Chief Engineer and Mr. Satoshi Shimizu, General Manager of Sumitomo Electric Device Innovations, Inc. for the valuable insights and suggestions they provided for this study.

Technical Terms

∗1 Gallium-nitride high-electron-mobility transistor (GaN-HEMT): A field-effect transistor with a high-mobility two-dimensional electron gas layer as a channel.

∗2 Raman spectroscopy: A method to investigate the distortion, measure the sample temperature, identify compounds and other physical properties using Raman scattering, which is generated by the interaction of the irradiated laser beam with molecular vibration or phonons. The spectrum is obtained by dispersing the Raman scattering light.

∗3 Inverse piezoelectric effect: Distortion of a polarized material when it is exposed to an electric field.

∗4 Knife-edge method: A method for determining the diameter of a laser beam from the change in its intensity when a shield having a linear edge (= knife-edge) is moved in the direction perpendicular to the optical axis of the beam.

References

(1) Y. Ohno, M. Akita, S. Kishimoto, K. Maezawa, and T. Mizutani, *Jpn, J. Appl. Phys.*, **vol. 41**, 452-454 (2002)
(2) T. Batten, J. W. Pomeroy, M. J. Uren, T. Martin, and M. Kuball, *J. Appl. Phys.,* **106**, 094509 (2009)
(3) K.Kosaka *et al., Shingaku Giho,* LQE2006-63 (2006)
(4) M. Kuball, A. Sarua, H. Ji, M. J. Uren, R. S. Balmer, and T. Martin, *2006 IEEE MTT-S International Microwave Symposium Digest.*, **vol. 4 of 5**, 1339-1342 (2006)
(5) K. R. Bagnall, C. E. Dreyer, D. Vanderbilt, and E. N. Wang, *J. Appl. Phys.*, **120**, 155104 (2016)
(6) Atlas User's Manual, Silvaco, Inc. (2016)
(7) A. Darwish, A. J. Bayba, and H. A. Hung, *IEEE Trans. Electron Devices*, **vol. 62**, no. 3, pp. 840-846 (Mar. 2015)
(8) J. C. Freeman and W. Mueller, *NASA/TM-2008-215444*
(9) K. R. Bagnall, *MIT Thesis*, Massachusetts Institute of Technology (2013)
(10) B. Raj and S. Bindra, *International Journal of Computer Applications*, **vol. 75**, no. 18 (2013)
(11) J. Piprek, *Semiconductor Optoelectronic Devices: Introduction to Physics and Simulation*, pp.141-144, Academic Press (2003)
(12) W. Liu and A. A. Balandin, *Appl. Phys. Lett.*, **vol. 85**, no. 22 (2004)

Contributors The lead author is indicated by an asterisk (*).

T. YONEMURA*
• Analysis Technology Research Center

M. FURUKAWA
• Assistant General Manager, Analysis Technology Research Center

S. MIZUNO
• Sumitomo Electric Device Innovations, Inc.

S. MATSUKAWA
• Group Manager, Analysis Technology Research Center

M. SHIOZAKI
• Senior Assistant General Manager, Analysis Technology Research Center

Y. NAMIKAWA
• Ph.D.
General Manager, Analysis Technology Research Center